International Journal of Engineering Trends and Technology
ISSN: 2231–5381 / https://doi.org/10.14445/22315381/IJETT-V73I11P125

Volume 73 Issue 11, 349-363, November 2025

Original Article

Customized Deep Learning Approach for Brain Tumor Classification

Vikram Verma[1,2], Alankrita Aggarwal[3]

[1]*Department of Computer Science and Engineering, Chandigarh University, Mohali, India.*
[2]*CSE Department, Panipat Institute of Engineering & Technology, Haryana, India.*
[3]*Department of Computer Science and Engineering, AIT, Chandigarh University, Mohali, India.*

[1]*Corresponding Author : mail4vikram@gmail.com*

Received: 23 January 2025 Revised: 11 November 2025 Accepted: 17 November 2025 Published: 25 November 2025

Abstract - *Magnetic Resonance Imaging (MRI) is widely accepted as the reference standard and a highly employed technique for brain tumor classification due to its ability to produce high-quality, non-invasive brain scans. Because tumor cells are heterogeneous, it is challenging to classify them; however, recent advancements in Machine Learning (ML) have enhanced the automation and accuracy of Brain Tumor Classification (BTC). Furthermore, with the expansion of artificial intelligence, particularly in Deep Learning (DL), a new avenue has opened, offering promising new opportunities for BT research and treatment. The objective of this research is to use multimodal images for the BTC. It specifically concentrates on MRI data collected from three different repositories. The novelty is in using these MRIs. Most of the earlier researches use single datasets or multiple datasets but applies DL individually. In this study, the MRI were mixed and then subjected to preprocessing before being used for training. The significant research gap is the absence of a unified framework for defining the most suitable neural network architecture for a given problem, which necessitates dependence on experimental trial-and-error strategies for new models. This study presents a Customized CNN (CCNN) solution for classifying 5712 brain MRI into four types. Besides CCNN, other Transfer Learning (TL) techniques like Custom VGG19 (C-VGG19), Customized MobileNet (C-MN), and customized DenseNet201 (C-DN201) are also used. According to trial data, test accuracy for the suggested CCNN was 95.80%, for C-VGG19 it was 97.02%, for C-MN it was 95.10%, and for C-DN201 it was 98.42%. DL frameworks utilizing CNN structures have been demonstrated to be highly effective for tumor classification and segmentation, successfully mitigating obstacles in MRI investigations.*

Keywords - *Brain Tumor, CNN, Deep Learning, Magnetic Resonance Imaging, Machine Learning.*

1. Introduction

Analysis of the brain is particularly challenging due to its billions of active cells. BT is becoming a leading cause of death in adults and children. Less than 2% of all cancers are primary BT, which affects roughly 300,000 people yearly throughout the world [1, 2]. People can develop more than 100 distinct types of BT [3]. To save human life, BTs must be properly graded and diagnosed as soon as possible. The high density of BTs makes the manual assessment awfully challenging.

For tumor detection, an automated computer-based approach is therefore highly advantageous [4]. Things are extremely different today. Radiologists can discover BT more rapidly by utilizing DL and ML [5]. More and more researchers involved in image processing and DL are working on creating precise and efficient algorithms for automated tumor classification. The efficacy of BT diagnosis using DL relies on efficient data handling. Handling large-scale data is crucial for creating accurate models, as it enables the storage, retrieval, and processing of massive medical imaging datasets. This capability is essential for building reliable DL models. A good data management system enables multimodal data integration, which combines data from various imaging modes, such as MRI and CT [3, 6]. Data augmentation gives a DL model a diversity of scenarios, which in turn helps it generalize better.

Furthermore, effective data management also involves creating and maintaining enhanced datasets to improve model performance [6].

This manuscript primarily concentrates on the following core research objectives.:

- The paper examines the latest advancements in BT identification systems, driven by ML and DL technologies, as detailed in Section 2.
- The research gaps have been systematically outlined in Section 3. This section serves as the foundation for

formulating the objectives and direction of the outlined framework.
- The paper explores the proposed and implemented framework in Section 4, highlighting the dataset, preprocessing procedures, and architecture.
- Section 5 gives a comprehensive examination of the experimental results.
- Lastly, Section 6 encapsulates the essential findings through a concise concluding summary.

2. Literature Review

In their article (2025), Mastoi et al used the concept of federated learning with GoogleNet. Their experiment was conducted on 7023 MRI taken from the Kaggle website. This method attained a 99.8% accuracy [7]. U-Net was used by Ilani et al. (2025) for BT classification. They used 3064 MRI from Figshare, categorized into 03 classes. Their method got 98.56% accuracy [8]. Islam et al (2024) used the EfficientNet family method for BT classification.

They used 3064 MRI from Figshare, categorized into 03 classes. Their method attained a 99.69% accuracy with EfficientNetB3 [9]. In 2024, Asiri et al. developed a hyper-tuned CNN framework for BT classification. They used 02 datasets. Both datasets were sourced from Kaggle. A total of 7,023 MRI spread across four classes constituted the first dataset. The second was a binary data set with 253 MRI. The authors reported an accuracy of 96.00% on the first data, while it was 88% on the second data [10].

Ahmed et al. (2023) utilized two pretrained networks - ResNet50 and InceptionV3 for classifying BT. They used 02 datasets. A total of 3459 MRI distributed across four classes constituted the first dataset obtained from Kaggle. The second data from Figshare was binary data having 3000 MRI. Their modified ResNet 50 achieved a 97.68 % accuracy, whereas modified Inception V3 got 96.25% on the first data. For the second dataset, they achieved 99.83% accuracy with ResNet50 and 98.22% with InceptionV3 [11].

In 2023, Mactina employed an innovative approach to identify brain tumors. This study utilized the SCARRL model, a meta-heuristic-based DL approach, to determine the malignancy or intermediate severity of BTs using MRIs. This model achieved a 98 percent accuracy [12]. Gupta et al. (2022) exploited Inception-ResNet-v2 as a pretrained model. Certain modifications were made to this, along with the addition of a Random Forest Tree to classify the BT.

The small dataset was enhanced using the Cyclic Generative Adversarial Networks (CGAN). The recommended model demonstrated an accuracy of 98.5% [13]. Díaz-Pernas (2021) utilized a deep CNN on MRI images to classify several forms of BT. The methodology employed a multipath CNN for enhanced performance. Stochastic Gradient Descent was employed for optimization. By utilizing this scheme, a remarkable accuracy of 97.3% was attained [14]. Semantic segmentation networks were created by Ruba et al. (2020) [9] using CNNs from MRI and CT scans. The GoogleNet CNN model was used in the suggested work. With respect to accuracy, this model demonstrated 99.6% accuracy, 99.6% sensitivity, 99.8% specificity, and 99.4% precision [15]. Abiwinanda et al. (2019) created a scheme utilizing CNN through DL methodologies for analyzing brain MR data.

In total, five classification models were created, and the second model demonstrated superior accuracy in classifying MR images. Within the proposed scheme, there is integration of the ReLU layer and the Max Pool layer, featuring a total of 64 hidden neurons. Under the training stage, the recommended model demonstrated an accuracy of 98.5%, while achieving an 84% accuracy during the validation phase [16].

Kabir Anaraki et al. (2019) devised a hybrid methodology that merged the evolutionary algorithm with CNN for categorizing BT. Their suggested method employed a genetic algorithm for selecting the structure of the CNN. This method has an accuracy of 90.9% [17]. The authors used four datasets.

These are IXI, REMBRANDT, TCGA-GBM, and a general hospital from Tehran. A novel categorization process is introduced by Afshar et al. (2019). Their work utilized the Capsule Network technique, also known as CapsNets. By adjusting the convolutional layer, this strategy improves the accuracy to 90.89% categorizing MR images of brain tumors.

According to the research, precision sees a notable 86.5% enhancement, specifically attributed to alterations within the convolution layer. Sixty-four feature map was used by CapsNets [18]. Seetha et al. (2018) used an automated framework.. The model employs a deep architecture with small convolutional kernels to enhance feature learning while maintaining low computational complexity. The adopted method gave an accuracy of 97.50% [19].

3. Research Gap

The absence of a unified framework for defining the most suitable neural network architecture for a given problem often necessitates dependence on experimental trial-and-error strategies. The tuning of critical hyperparameters-like learning rate and hidden layer size-continues to depend on heuristic experimentation rather than established theoretical or automated principles. Overfitting remains a persistent challenge for deep learning models across diverse datasets, necessitating advanced approaches to enhance regularization and generalization capabilities. The internal mechanisms through which deep learning models analyse input data and produce outputs remain largely opaque, underscoring the need for explainable AI approaches. Table 1 gives a summary of several other relevant research works.

Table 1. Summary of procedures used for BT classification

Year	Ref No.	Technique	Data repository	Images used	Accuracy %	Remark (Tumor classes identified)
2025	[20]	Xception with Transfer learning	Kaggle	7023	98.73	3 (Meningioma, Glioma, Pituitary)
2025	[21]	Attention-based GoogLeNet-style CNN	Figshare	3064	97.62	3 (Meningioma, Glioma, Pituitary)
2025	[22]	ADE Algorithm and Diet Transformer	Kaggle	5249	96.09	3 (Meningioma, Glioma, Pituitary)
2024	[23]	InceptionV4	Kaggle	7022	98.70	3 (Meningioma, Glioma, Pituitary)
2023	[24]	Vision Transformer (ViT)	BraTS 2018	1425	96.75	3 (Glioma, Meningioma, Pituitary)
2023	[25]	IVX16 ensemble of VGG16, InceptionV3, and Xception	Kaggle	3264	96.94	3 (Meningioma, Glioma, Pituitary)
2022	[26]	GoogLeNet	Br35H Kaggle	3000	99.51	Tumor or non-tumor
2021	[27]	EfficientNet	Figshare	3064	98.04	3 (Meningioma, Glioma, Pituitary)
2021	[28]	Fine-tuned Inception-v3	Figshare	3064	94.34	3 (Meningioma, Glioma, Pituitary)
2020	[29]	Convolutional NADE	Figshare	3064	95.00	3 (Meningioma, Glioma, Pituitary)
2019	[30]	GoogLeNet Transfer Learning Softmax	Figshare	3064	98.0	3 (Meningioma, Glioma, Pituitary)
2019	[31]	ResNet - 101	Figshare	3064	93.83	3 (Meningioma, Glioma, Pituitary)
2018	[32]	DenseNet-LSTM	Figshare	3064	92.13	3 (Meningioma, Glioma, Pituitary)

4. DL Methodology for Classification

4.1. Customization of the Architectures Used

Four models form the basis of this study: (a) Customised CNN (CCNN), (b) Customized VGG-19 (C-VGG19), (c) Customised MobileNet (C-MN), d) customised DenseNet201 (C-DN201) techniques. The proposed customized CNN (CCNN) architecture, Figure 1, is an efficient DL model for high-resolution medical image classification. It incorporates three convolutional stages with 5×5, 5×5, and stacked 3×3 kernels. Batch Normalization (BN) and the SAF are applied following each convolution to ensure stable gradient flow [33]. Residual skip connections using 1×1 convolutions are employed to enhance feature reuse and mitigate vanishing gradients. This block is named as Residual Convolutional Block (RCB) [16]. A Dual-Pooling Swish-Activated Classification Head (DSCH) is appended after the final RCB. The module incorporates a 1×1 convolution for channel refinement. It is followed by Global Average Pooling (GAP) for capturing overall contextual information [34]. This stage operates in parallel with Global Max Pooling (GMP) to highlight the most discriminative features within the image. The concatenation (GAP + GMP) enhances feature diversity and improves class discrimination. This concatenated feature vector is processed through a dense layer (128 neurons) along with SAF and 50% dropout regularization to enhance generalization. After that, it is again passed through a second dense layer with 4 output neurons and a 40% dropout rate. The vector thus generated is passed through a Softmax layer [35, 36]. This Softmax generates class probabilities for final classification. The proposed customized VGG-19 model, Figure 2, enhances the original architecture by integrating BN, SAF, and residual connections with 1×1 convolutions before each max-pooling layer to improve gradient flow and training stability [37]. A lightweight DSCH replaces the traditional fully connected layers. This design achieves improved accuracy, faster convergence, and reduced computational complexity compared to the conventional VGG-19 [38]. The proposed customized MobileNet architecture, Figure 3 is designed to enhance feature representation and classification accuracy for high-resolution medical imagery. The model extends the conventional MobileNet by incorporating deeper Depthwise Separable Convolution (DS) blocks, enabling effective multi-scale feature extraction while maintaining computational efficiency [39]. A 1×1 convolutional bottleneck layer is introduced for efficient feature compression, reducing redundancy and improving discriminative capability. Furthermore, DSCH is employed to capture both average contextual and dominant spatial activations, providing a more comprehensive feature embedding [12]. Overall, the customized MobileNet strikes the ideal balance between high-fidelity feature learning and processing economy. This makes it well-suited for precise BTC tasks [20].

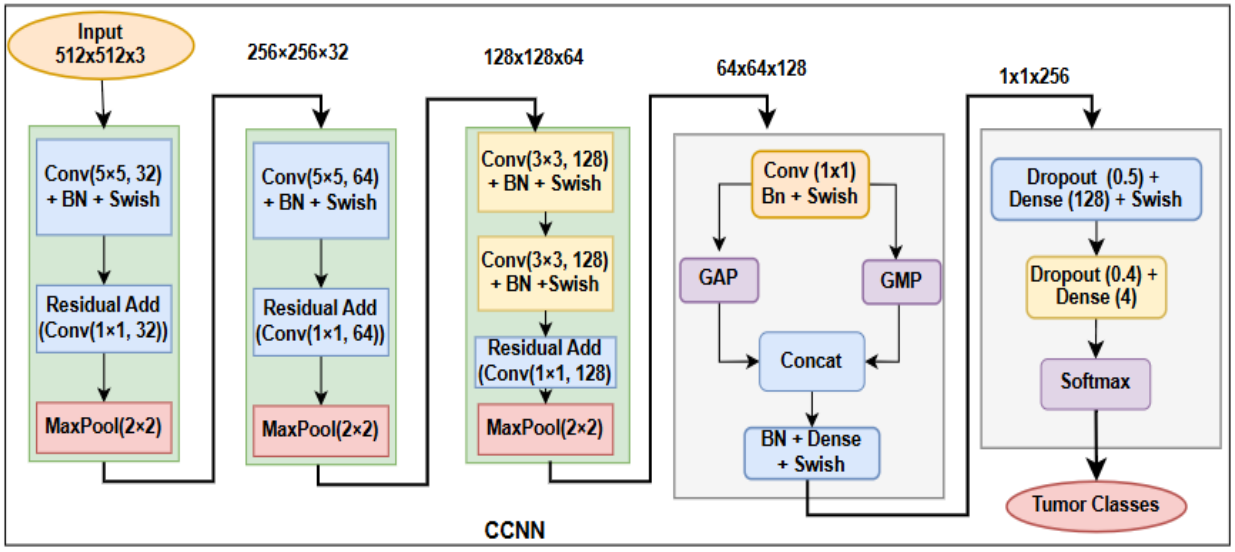

Fig. 1 CCNN architecture

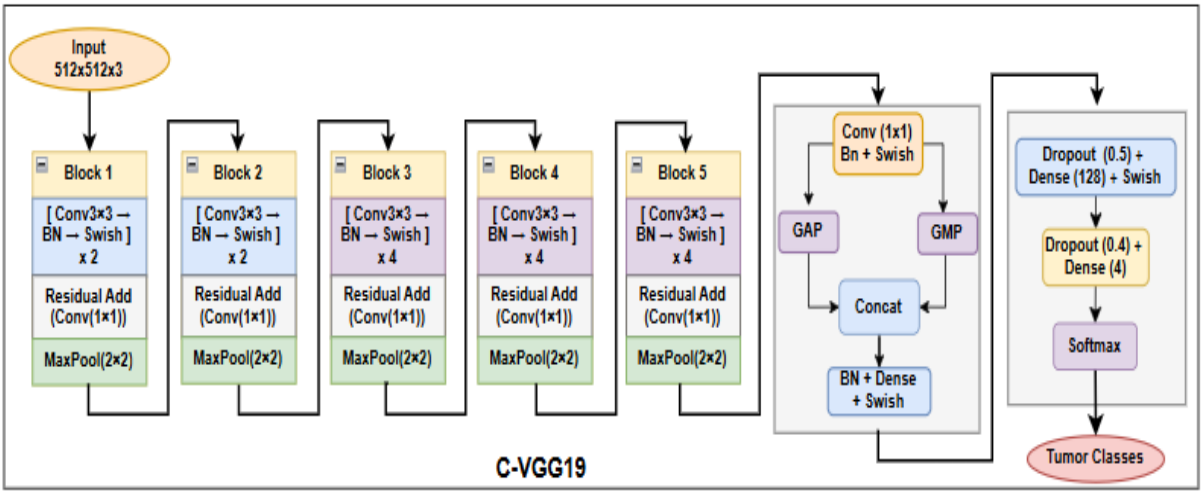

Fig. 2 C-VGG19 architecture

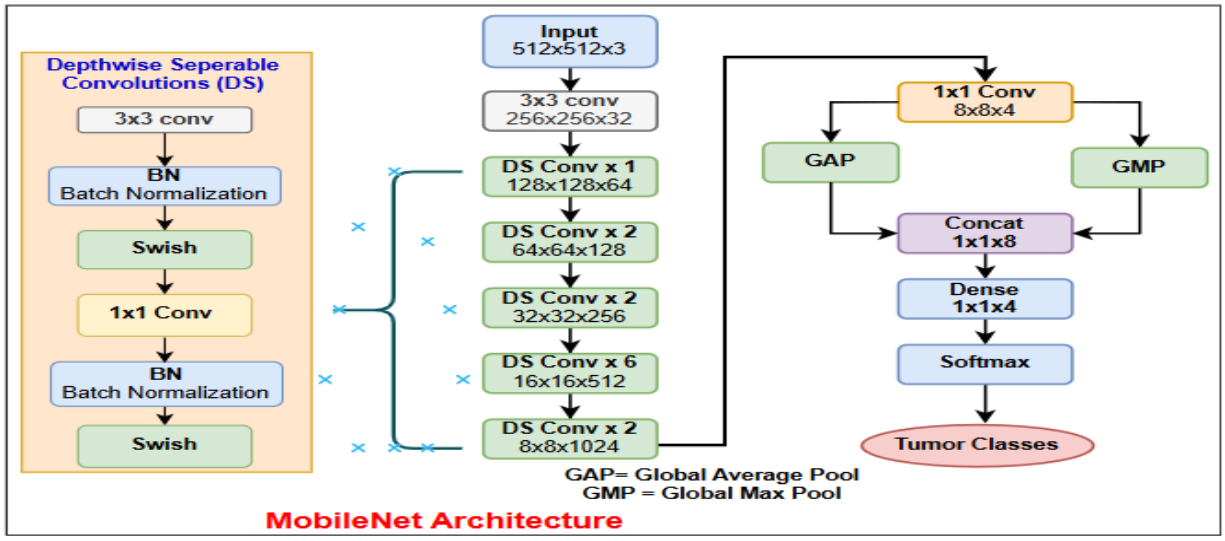

Fig. 3 C-MN architecture

Figure 4(a) exhibits a customized DenseNet-inspired architecture with notable deviations from standard configurations. It begins with a 7×7 convolution followed by BN, SAF, and a residual 1×1 convolution before max-pooling. The network retains the DenseNet-201 configuration with a growth rate of k = 32 and a non-standard layer progression of [6, 12, 48, 32]. The proposed C-DN201 integrates a dual-stage bottleneck structure, where an additional pair of 1×1 convolutions following the final dense block performs progressive channel compression (1920 to 512 to 256). Doing this enhances feature compactness and discrimination prior to global pooling. Finally, DSCH is then applied to capture both average contextual and salient activations for robust tumor discrimination.

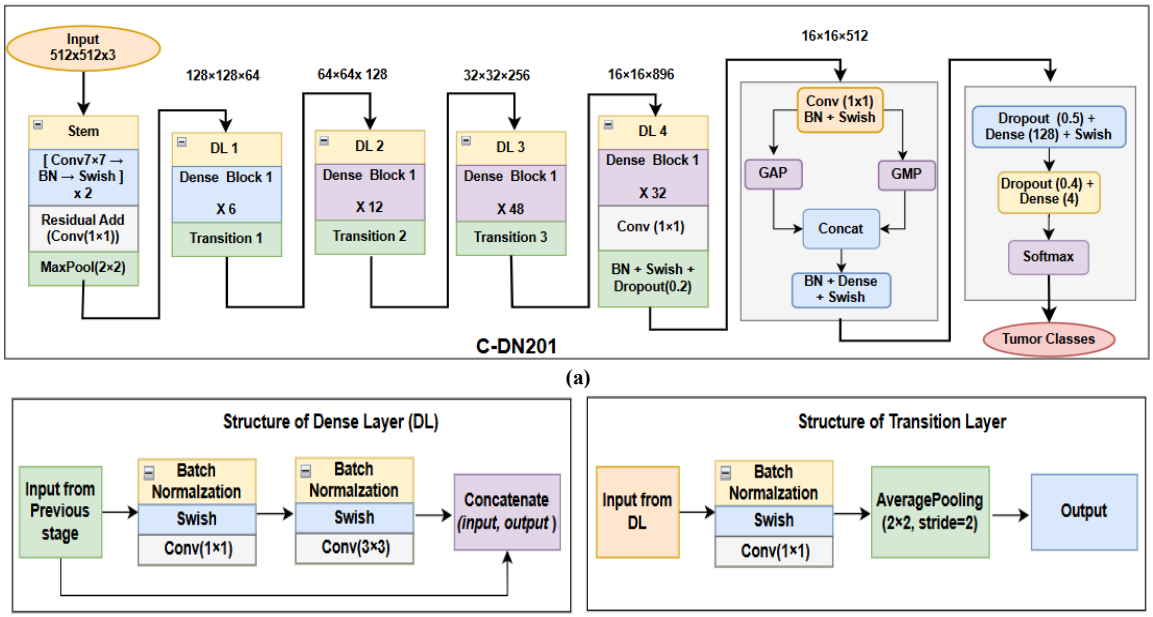

Fig. 4(a) C-DN201 architecture, and (b) Dense layer, and (c) Transition layer.

4.2. Mining the Data

To gather image modality from various sources that will be needed to feed the detection machine for the purpose of tumor detection [8]. The MRI were sourced from the Kaggle website [40-42].

The dataset underwent a meticulous cleaning process aimed at removing noisy, misclassified, and degraded images, resulting in a more consistent and reliable dataset.

This dataset has 5718 MRI. The data was divided into three clusters. The first group of 4005 MRI is utilized for training, whereas the second group of 1142 MRI is for validation. An unseen dataset of 571 MRI was used for testing. Table 2 summarizes the dataset.

Table 2. Summary of the dataset Used

MRI	Train set	Validation set	Test set	Total
Glioma	931	263	132	1325
Meningioma	938	268	134	1340
No tumor	1113	318	159	1590
Pituitary	1023	293	146	1462
Total	4005	1142	571	5718

4.3. Data Preparation

In the clinical setting, the quality and quantity of imaging are essential for generating a reliable diagnosis. The actual MRI may contain numerous unneeded and superfluous details [43]. Due to its signal sensitivity, noise is hard to eliminate [4, 37]. To preserve the original visual qualities, pre-processing methods like filtration are applied. MRI were subjected to a standardized preprocessing pipeline to improve image quality, contrast, and consistency across the dataset [5, 9, 23]. The procedure utilized SimpleITK-based filtering and Gaussian smoothing to suppress noise while preserving anatomical structures [44] effectively. Figure 5 depicts the noisy MRI and the preprocessed, denoised image.

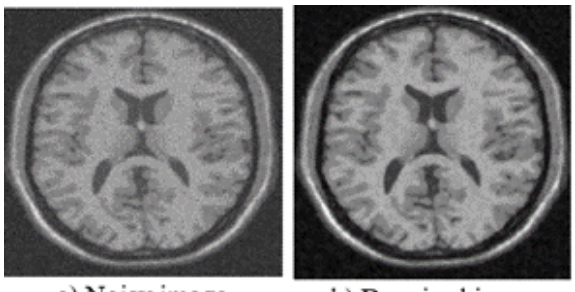

Fig. 1 (a) Noisy MRI, and (b) Preprocessed denoised image.

A light morphological erosion was applied to remove small unwanted artifacts and refine region boundaries [38]. To achieve uniform intensity scaling across scans, z-score normalization was employed, minimizing inter-patient and inter-scanner variability. Finally, CLAHE enhanced local contrast and emphasized tumor regions without amplifying background noise. This standardized preprocessing ensured high-quality, normalized inputs, enabling reliable and accurate model training. Every MRI was altered to have the same dimensions.

4.4. Data Augmentation

The performance of DL algorithms is intrinsically tied to the relevance, volume, and quality of training data [5, 17]. Unfortunately, the lack of sufficient data remains a major barrier, as gathering useful datasets is often an expensive and labour-intensive process. To overcome this obstacle, data augmentation approaches have been used. Training data undergoes a three-step image augmentation procedure. The first augmentation involves a single rotation of +10°, representing minor variations in patient positioning during image acquisition. The 2nd augmentation consisted of a horizontal flip, which introduced mirror symmetry and reduced orientation bias in the dataset. The third augmentation combined a mild zoom factor of 0.95× with a gamma correction factor of 1.1. This third step simulates subtle variations in acquisition scale and scanner-specific intensity distribution [45]. The augmented set now comprises 11,994 MRI. This augmentation protocol generated three additional samples per image, effectively quadrupling the dataset size to 15992 images.

4.5. Methodology

Four models form the basis of this study. Customised Transfer Learning (CTL) has been implemented across three frameworks, namely C-MN, C-VGG19, and C-DN201, to enhance classification performance.

Figure 6 shows the CCNN model. A customized model for tumor detection is specifically designed for BTC. The modification involves adjusting hyperparameters to accommodate the nuances of BT structures. The CCNN consists of alternating Conv2D layers and MaxPooling2D as depicted in Figure 1.

The SAF exhibits a smooth, non-monotonic response that facilitates efficient gradient propagation and enhances convergence stability compared to conventional ReLU. Owing to its self-gating characteristic, Swish preserves minor negative activations, thereby improving feature expressiveness and contributing to superior overall network performance [46].

For improving prediction accuracy, the categorical cross-entropy was used. This is a loss function that compares the real and predicted class probabilities, ensuring effective optimization for multi-class classification tasks [13]. Label smoothing was employed to prevent the model from becoming overconfident by slightly softening the target class distributions during training [47]. This technique enhances generalization and improves robustness by mitigating overfitting to hard one-hot labels.

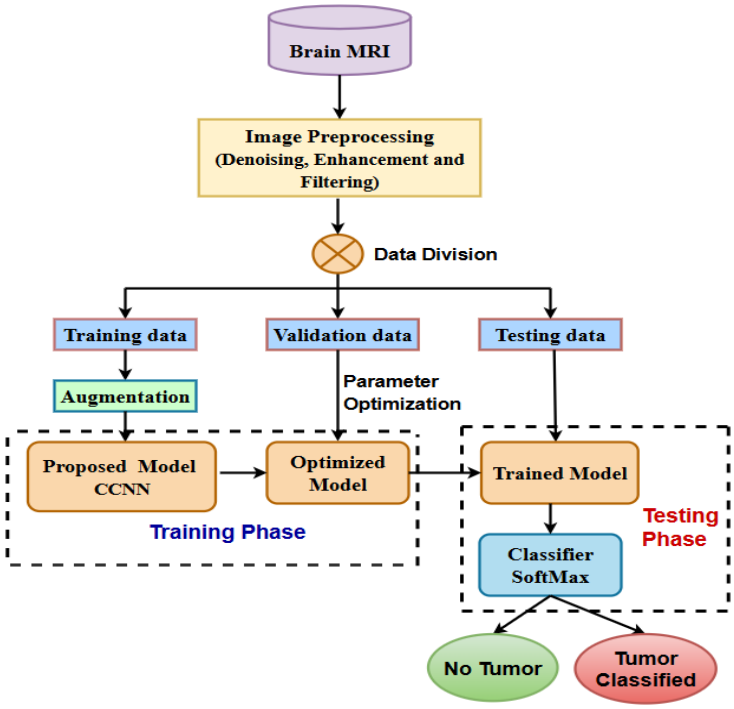

Fig. 6 CCNN methodology for classification of BT

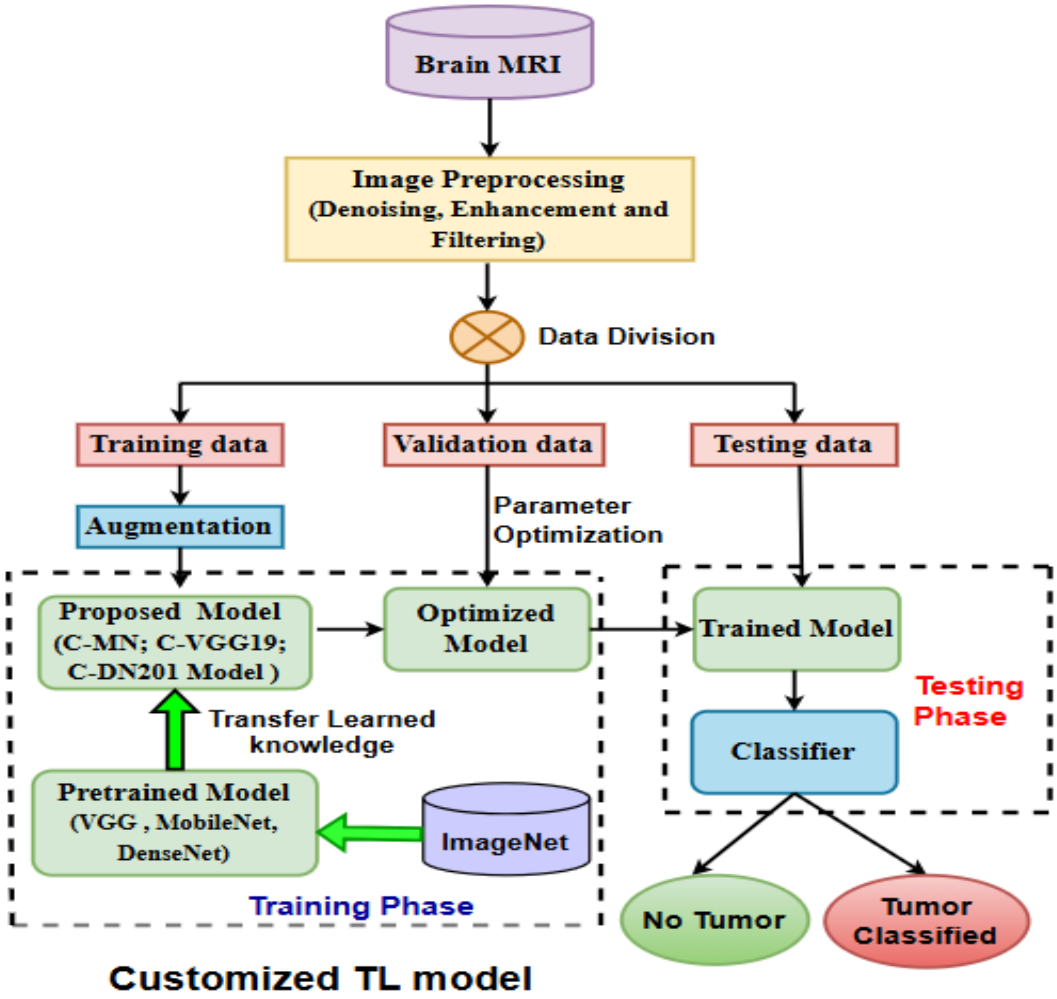

Fig. 7 CTL Scheme for classification of BT

The three CTL used are C-VGG19, C-MN, and C-DN201. The customization is achieved by modifying the framework, as previously discussed in Figures 2-4 The goal is to control the robustness and knowledge of the pre-trained model while enhancing its performance. Figure 7 represents CTL. Transfer Learning takes advantage of the information contained in prior models. This work extracts features from MR pictures using pre-learned weights from model training on the ImageNet dataset [6].

4.6. Training and Testing

Separate data cluster are utilized for trining, validation, and testing. During model development, the validation set aids in performance monitoring and hyperparameter optimization [13, 16]. Eighty epochs were used to train each model. We used Early Stopping to monitor the validation loss and prevent overfitting. The best model weights were restored automatically once the validation performance ceased to improve. The patience level of 10 epochs was used. All the architectures employed Nadam as an optimiser. Regularization is applied with a Dropout layer, which arbitrarily sets 45% of the inputs to zero through training. This system improves generalization on unseen data. The concept of Multi-Layer Perceptron (MLP) in Customised TL allowed us to leverage the powerful feature extraction capabilities of pre-trained convolutional networks while tailoring the classifier specifically to our dataset, resulting in faster convergence during training [21]. For training, the Hyper parameter as used are provided in Table 3.

Table 3. Hyperparameters for mode l training

Parameter	Value
Epoch	80
Learning Rate	0.0012
Loss Function	Categorical cross-entropy
Batch size	32
Optimizer	Nadam
Dropout	0.45
Activation	Swish
Momentum	0.90
Classifier	Softmax

5. Results and Discussion

5.1. CCNN Model

Figures 8(a) and 8(b) show the accuracy and loss trends for the CCNN algorithm. Given the small gap between the curves, it appears to be generalizing effectively. The training accuracy of 98.83% achieved by the CCNN model, together with the validation accuracy of 96.17%, indicates efficient learning behavior and minimal signs of overfitting. The CCNN model exhibits rapid loss convergence during the early epochs, with both training and validation losses stabilizing at low values, indicating effective optimization and a strong generalization capability. Figure 9 illustrates the CM, which visualizes the potency of the CCNN model. It compares the actual values of a dataset with the forecasted values generated by the CCNN. The CCNN performs well overall, with high numbers of correct classifications in each class. The most common misclassifications occur between Glioma and Meningioma, which could indicate similarities between these two classes that make them harder to distinguish.

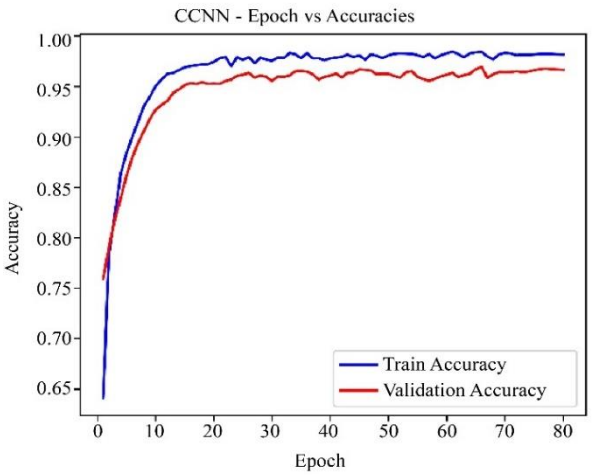

Fig. 8(a) CCNN accuracy plots

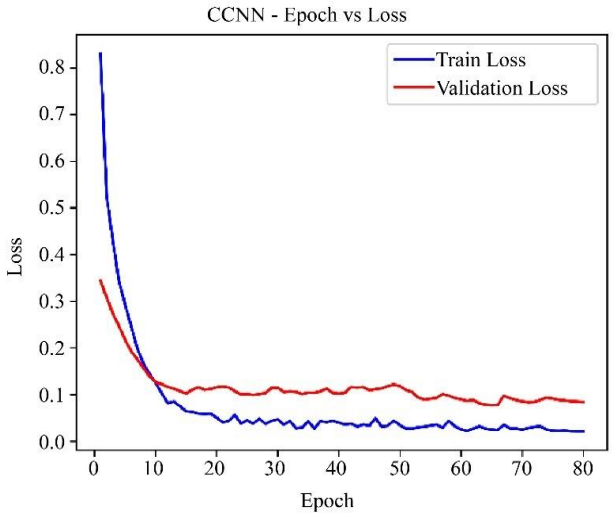

Fig. 8(b) CCNN loss plots

Table 4. Class accuracy of CCNN model

Tumor Class	Test Accuracy	Specificity
Glioma tumor	0.9667	0.9818
Meningioma	0.9545	0.9680
No tumor	0.9912.	0.9951
Pituitary tumor	0.9895	0.9906

The classes “NO Tumor” and “Pituitary Tumor” have fewer misclassifications, suggesting they are more distinct and easier to classify correctly. Report in Table 5 gives an appraisal of the model in predicting the diverse tumors.

No tumor and Pituitary tumor demonstrate a high metrics score, indicating robust performance in correctly identifying instances of these tumor types. Meningioma shows slightly lower scores, particularly in recall, suggesting some difficulty in accurately capturing all instances of this tumor class.

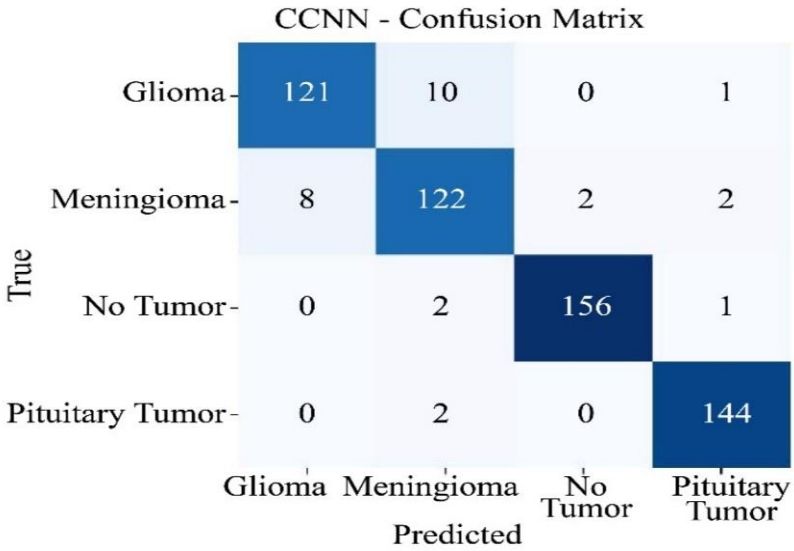

Fig. 9 CM for CCNN

Table 5. Class report CCNN model

Tumor Class	Precision	Recall	F1 score	Support
Glioma tumor	0.9380	0.9167	0.9272	132
Meningioma	0.8971	0.9104	0.9037	134
No tumor	0.9873	0.9811	0.9842	159
Pituitary tumor	0.9730	0.9863	0.9796	146

5.2. C-VGG19 Model

Figures 10(a) and 10(b) show the accuracy and loss trends for the C-VGG19 framework. The accuracy is 99.12% during training, whereas it is 97.87% during validation. Table 6 provides the C-VGG19's test specificity and accuracy. It is evident that the C-VGG19 realizes very respectable results across all BTC.

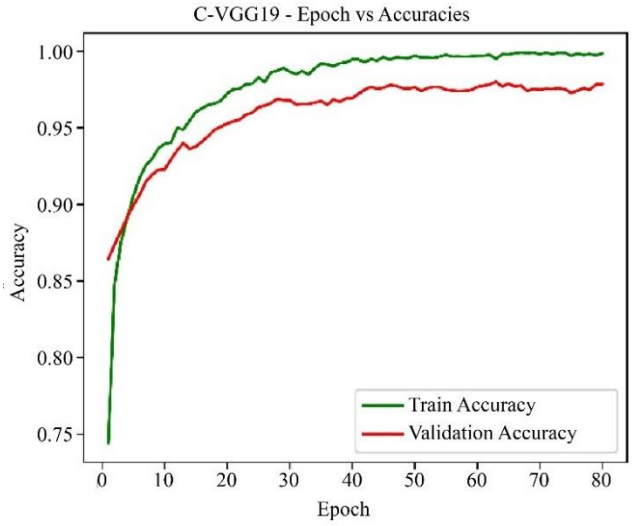

Fig. 10(a) C-VGG19 accuracy plots

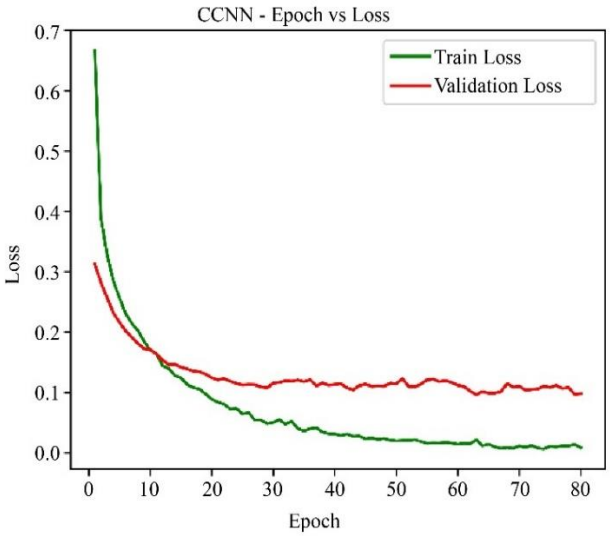

Fig. 10(b) C-VGG19 loss plots

Figure 11 depicts the CM of the C-VGG19 model. The CM for the BT classification shows high accuracy for all classes with minimal misclassifications.

The report in Table 7 gives an appraisal of the model in predicting the diverse tumors. The model is particularly effective at identifying cases with no tumors, as indicated by the highest precision and recall in this category.

Table 6. Class accuracy of C-VGG19 model

Tumor Class	Test Accuracy	Specificity
Glioma tumor	0.9842	0.9909
Meningioma	0.9772	0.9863
No tumor	0.9912	0.9927
Pituitary tumor	0.9877	0.9906

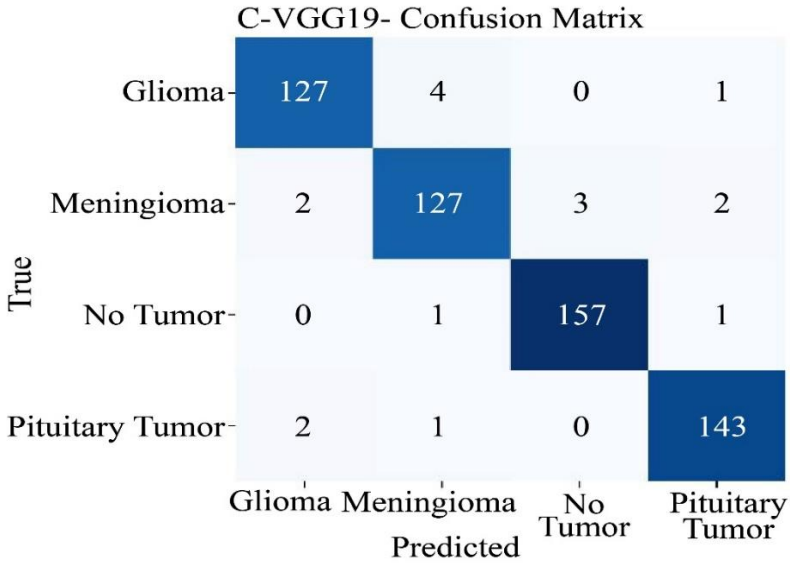

Fig. 11 CM for C-VGG19

Table 7. Class report C-VGG19 model

Tumor Class	Precision	Recall	F1 score	Support
Glioma tumor	0.9695	0.9621	0.9658	132
Meningioma	0.9549	0.9478	0.9513	134
No tumor	0.9812	0.9874	0.9843	159
Pituitary tumor	0.9728	0.9795	0.9761	146

5.3. C-MN Model

The C-MN model's accuracy and loss trends are shown in Figures 12 (a) and (b). The model is generalizing nicely, as seen by the curves. The training accuracy is 98.75%, whereas the validation accuracy is 96.26%. Table 8 provides the C-MN's test specificity and accuracy.

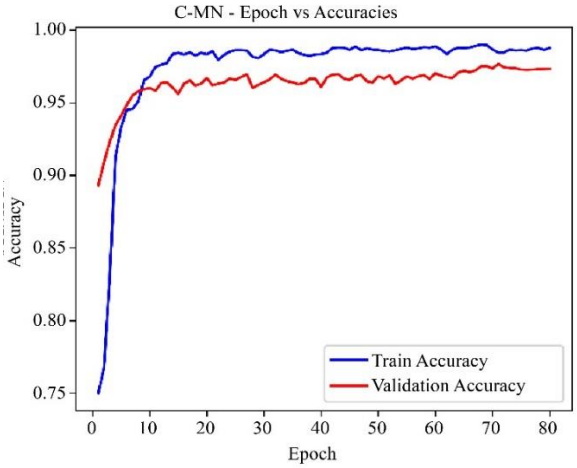

Fig. 12(a) C-MN accuracy plots

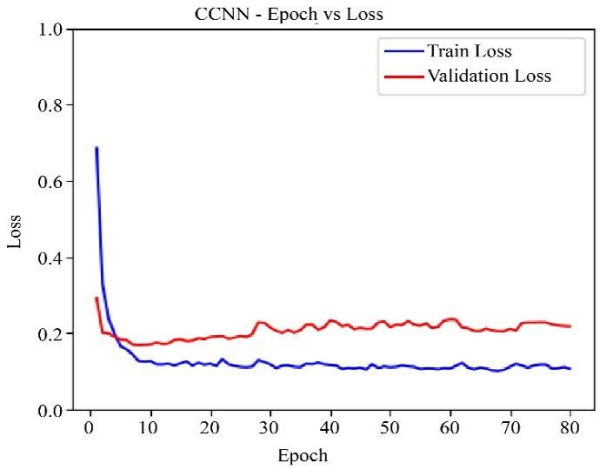

Fig. 12(b) C-MN loss plots

The table indicates robust performance and reliability in distinguishing between different tumor types. Figure 13 depicts the CM that visualizes the potency of the C-MN model. The CM report in Table 9 shows that neither tumor nor pituitary tumor has a high score, indicating robust performance in correctly identifying instances of these tumor types.

Table 8. Class accuracy of C-MN model

Tumor Class	Test Accuracy	Specificity
Glioma tumor	0.9737	0.9818
Meningioma	0.9615	0.9748
No tumor	0.9895	0.9976
Pituitary tumor	0.9912	0.9906

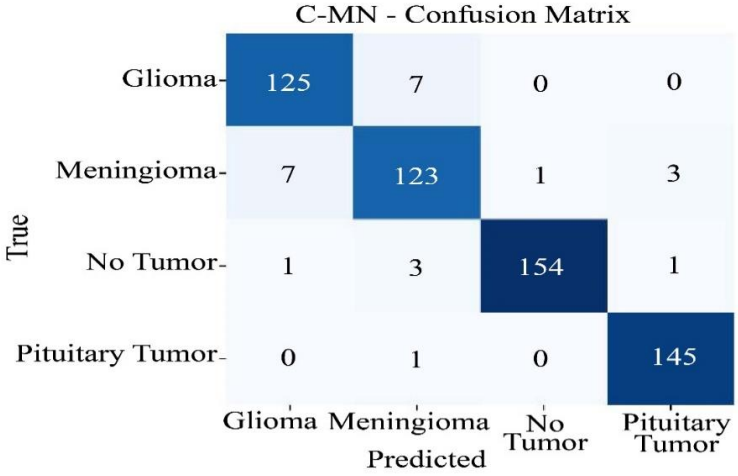

Fig. 13 CM for C-MN

Table 9. CLASS report C-MN model

Tumor Class	Precision	Recall	F1 score	Support
Glioma tumor	0.9398	0.9470	0.9434	132
Meningioma	0.9179	0.9179	0.9179	134
No tumor	0.9935	0.9686	0.9809	159
Pituitary tumor	0.9732	0.9932	0.9831	146

5.4. C-DN201 Model

Figure 14 (a) and 14 (b) depict the accuracy and loss trends for the C-DN201. A small variation in the curves advocates that it is generalizing significantly. The train accuracy is 99.25% whereas it is 98.58% during validation.

The C-DN201 model exhibits rapid loss convergence within the early epochs, with both training and validation losses stabilizing at low values, indicating effective optimization and a strong generalization capability.

Table 10 presents the class-wise performance of the C-DN201 model in terms of test accuracy and specificity across various tumor categories.

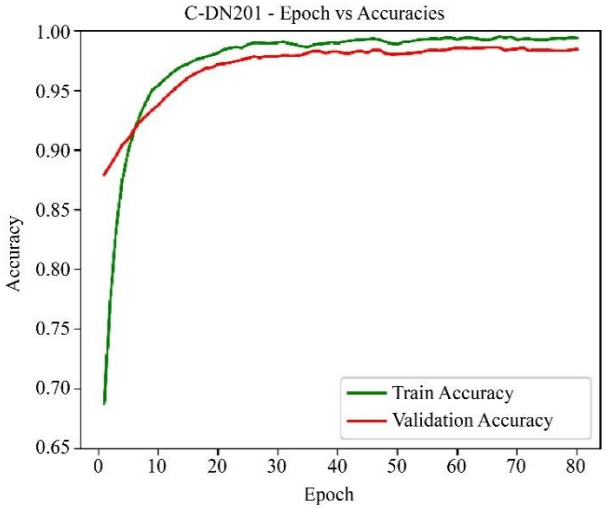

Fig. 14(a) C-DN201 accuracy plots

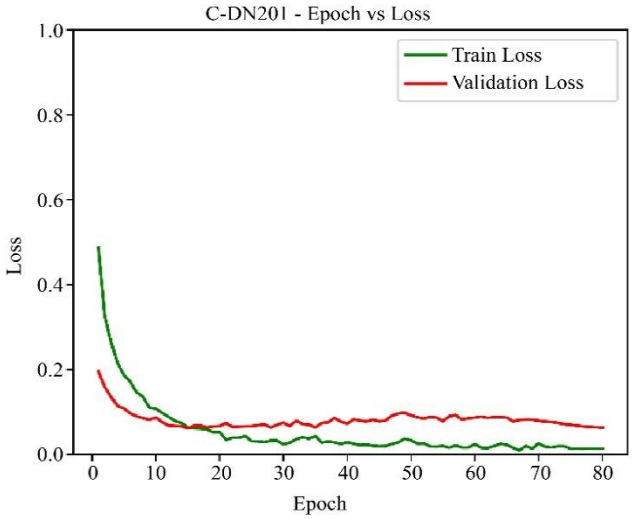

Fig. 14(b) C-DN201 loss plots

Table 10. Class accuracy Of C-DN201 model

Tumor Class	Test Accuracy	Specificity
Glioma tumor	0.9930	0.9954
Meningioma	0.9912	0.9954
No tumor	0.9947	0.9951
Pituitary tumor	0.9965	0.9976

Figure 15 depicts the CM that visualizes the potency of the C-DN201 model. High precision and recall scores indicate that the C-DN201 performs exceptionally well across all classes. Overall, the C-DN201 model demonstrates strong capability with slight misclassifications. Such a level of effectiveness implies that the C-DN201 model is appropriate for real-world use in classifying various BT types.

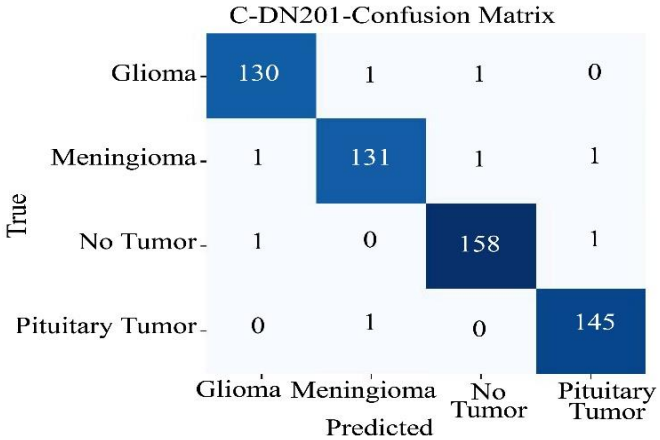

Fig. 15 CM for C-DN201

The report derived from the CM is in Table 11, which gives an appraisal of the C-DN201 model in predicting the diverse tumors. The Matthews Correlation Coefficient (MCC) is widely regarded as a dependable indicator for evaluating the overall quality of classification algorithms [48]. Unlike simple accuracy, MCC incorporates all four outcomes of the CM (TP, TN, FP, and FN), thereby delivering a fair and unbiased measure of a model's predictive capability, especially in cases of class imbalance. As presented in Table 12, the C-DN201 model recorded the highest MCC value of 0.9836, demonstrating a strong correlation between its predicted and actual outcomes. This high score reflects the model's

robustness and consistent learning behaviour throughout the training and testing phases. The same pattern can be observed in Figure 17, where C-DN201 maintains a clear lead over the other models in overall performance. The steady improvement across all evaluation parameters highlights DN20's enhanced capability to generalize well, minimize misclassifications, and deliver more accurate predictions for brain tumor classification tasks.

Table 11. CLASS report C-DN201 model

Tumor Class	Precision	Recall	F1 score	Support
Glioma tumor	0.9848	0.9848	0.9848	132
Meningioma	0.9850	0.9776	0.9813	134
No tumor	0.9875	0.9937	0.9906	159
Pituitary tumor	09932	0.9932	0.9932	146

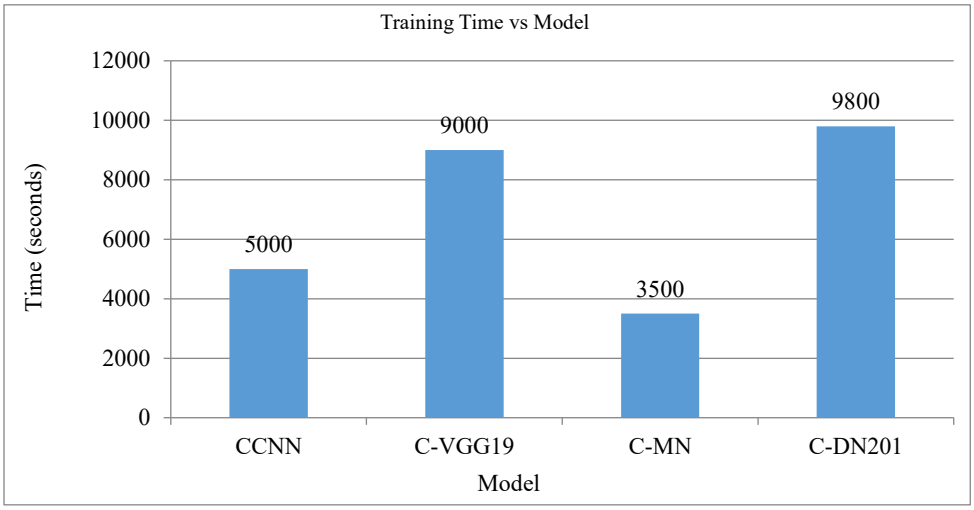

Fig. 16 Training time vs Model graph

Table 12. Performance report

Metrics	CCNN	C-MN	C-VGG19	C-DN201
Macro Precision	0.9488	0.9561	0.9696	0.9876
Macro Recall	0.9486	0.9566	0.9692	0.9873
Macro Dice	0.9487	0.9563	0.9694	0.9875
Test Accuracy	0.9510	0.9580	0.9702	0.9877
MCC	0.9345	0.9439	0.9602	0.9836

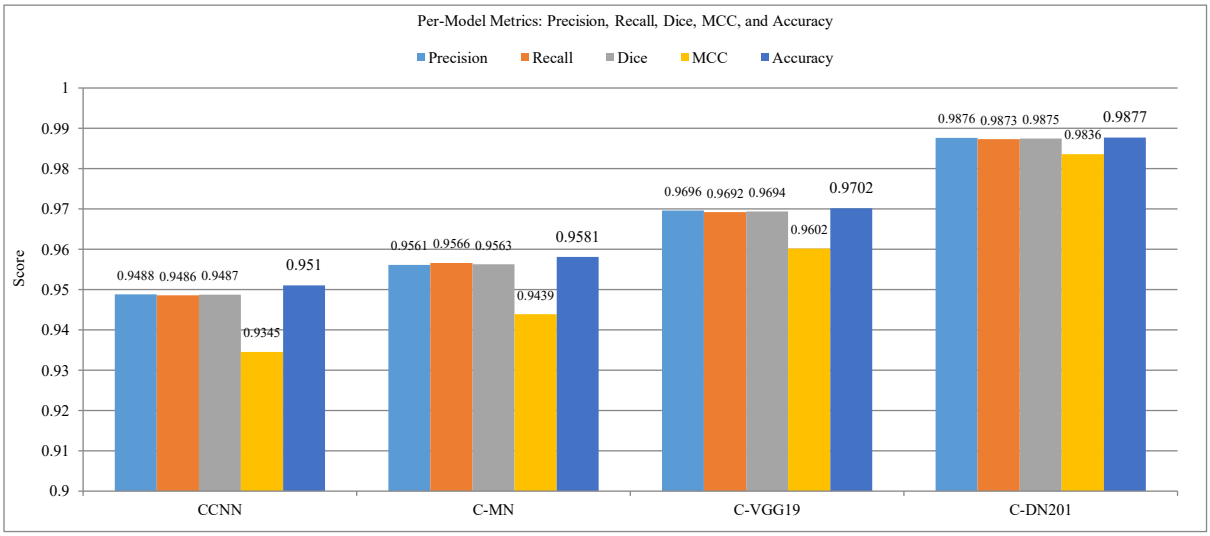

Fig. 17 Per model comparison

6. Conclusion

This study presents a comprehensive framework for classifying BTs, beginning with a meticulous data collection process. Prior to model training, the data is thoroughly organized, pre-processed, and augmented to achieve improved generalization and robustness.

The classification report compares the performance of four different classification methods (CCNN, C-MN, C-VGG19, C-DN201) across four BT classes. Method C-DN201 consistently achieves the highest efficacy across all BT classes, demonstrating excellent performance with nearly perfect scores, especially for Pituitary tumor with an overall metric score of 0.9932. Method C-VGG19 also shows strong performance with high metrics across the board, particularly for No tumor and Glioma tumor.

Methods CCNN and C-MN exhibit slightly lower performance compared to C-DN201 and C-VGG19, with Method CCNN having the lowest recall for the Glioma tumor (0.9167) and Meningioma (0.9104). Method C-MN shows variability in its metrics but generally maintains high precision and recall. Overall, Method C-DN201 is the most effective, followed closely by C-VGG19, while CCNN and C-MN are slightly less consistent but still perform well.

The proposed approach makes a valuable contribution to the field of medical data analysis. Moreover, this applied research study is expected to provide significant assistance and practical benefits to radiologists in clinical decision-making. By obtaining a second opinion, radiologists will be better able to identify the types, positions, diameters, and intensities of tumors.

Acknowledgment

Thanks to our families and colleagues who supported us morally.

Author Contributions

Conceptualization, methodology, and investigation V.V.; writing the original draft, V.V.; review and editing, V.V. and A.A.; Both authors have read and agreed to the published version of the manuscript.

Data Availability Statement

The data used in this study are openly available on Kaggle and Figshare.

Abbreviations

BT	Brain tumor
BTC	Brain Tumor Classification
ML	Machine Learning
DM	Data Management
DL	Deep Learning
DLM	Deep Learning Model
CLAHE	Contrast Limited Adaptive Histogram Equalization
DSCH	Dual-pooling Swish-activated classification head
CNN	Convolutional Neural Networks
CCNN	Customized CNN
C-VGG19	Customized VGG19
C-MN	Customized MobileNet
C-DN201	Customized DenseNet201
CM	Confusion Matrix
MRI	Magnetic Resonance Imaging
TL	Transfer Learning
SAF	Swish Activation Function

References

[1] Arati Rath et al., "A Bibliometric Review: Brain Tumor Magnetic Resonance Imagings using Different Convolutional Neural Network Architectures," *World Neurosurgery*, vol. 170, pp. e681-e694, 2023. [CrossRef] [Google Scholar] [Publisher Link]

[2] Global Cancer Observatory, Cancer Today, International Agency for Research on Cancer, 2024. [Online]. Available: https://gco.iarc.fr/en

[3] Bjoern H. Menze et al., "The Multimodal Brain Tumor Image Segmentation Benchmark (BRATS)," *IEEE Transactions on Medical Imaging*, vol. 34, no. 10, pp. 1993-2024, 2015. [CrossRef] [Google Scholar] [Publisher Link]

[4] Ashwini Pradhan et al., "On the Classification of MR Images using 'ELM-SSA' Coated Hybrid Model," *Mathematics*, vol. 9, no. 17, pp. 1-21, 2021. [CrossRef] [Google Scholar] [Publisher Link]

[5] Annapareddy V.N. Reddy et al., "Analyzing MRI Scans to Detect Glioblastoma Tumor using Hybrid Deep Belief Networks," *Journal of Big Data*, vol. 7, no. 1, pp. 1-17, 2020. [CrossRef] [Google Scholar] [Publisher Link]

[6] Dillip Ranjan Nayak et al., "Brain Tumour Classification using Noble Deep Learning Approach with Parametric Optimization through Metaheuristics Approaches," *Computers*, vol. 11, no. 1, pp. 1-14, 2022. [CrossRef] [Google Scholar] [Publisher Link]

[7] Qurat-Ul-Ain Mastoi et al., "Explainable AI in Medical Imaging: An Interpretable and Collaborative Federated Learning Model for Brain Tumor Classification," *Frontiers in Oncology*, vol. 15, pp. 1-16, 2025. [CrossRef] [Google Scholar] [Publisher Link]

[8] Mohsen Asghari Ilani, Dingjing Shi, and Yaser Mike Banad, "T1-Weighted MRI-Based Brain Tumor Classification using Hybrid Deep Learning Models," *Scientific Reports*, vol. 15, no. 1, pp. 1-16, 2025. [CrossRef] [Google Scholar] [Publisher Link]

[9] Md. Manowarul Islam et al., "BrainNet: Precision Brain Tumor Classification with Optimized Efficient Net Architecture," *International Journal of Intelligent Systems*, vol. 2024, no. 1, pp. 1-24, 2024. [CrossRef] [Google Scholar] [Publisher Link]

[10] Abdullah A. Asiri et al., "Enhancing Brain Tumor Diagnosis: An Optimized CNN Hyperparameter Model for Improved Accuracy And Reliability," *PeerJ Computer Science*, vol. 10, pp. 1-28, 2024. [CrossRef] [Google Scholar] [Publisher Link]

[11] Syed Ahmmed et al., "Enhancing Brain Tumor Classification with Transfer Learning across Multiple Classes: An In-Depth Analysis," *BioMedInformatics*, vol. 3, no. 4, pp. 1124-1144, 2023. [CrossRef] [Google Scholar] [Publisher Link]

[12] Josephine Nijofi Mactina, and S. Neduncheliyan, "An Towards Efficient Optimal Recurrent Neural Network-Based Brain Tumour Classification using Cat and Rat Swarm (CARS) Optimisation," *Multimedia Tools and Applications*, vol. 83, no. 10, pp. 30897-30918, 2023. [CrossRef] [Google Scholar] [Publisher Link]

[13] Rajeev Kumar Gupta et al., "Brain Tumor Detection and Classification Using Cycle Generative Adversarial Networks," *Interdisciplinary Sciences: Computational Life Sciences*, vol. 14, no. 2, pp. 485-502, 2022. [CrossRef] [Google Scholar] [Publisher Link]

[14] Francisco Javier Díaz-Pernas et al., "A Deep Learning Approach for Brain Tumor Classification and Segmentation using a Multiscale Convolutional Neural Network," *Healthcare*, vol. 9, no. 2, pp. 1-14, 2021. [CrossRef] [Google Scholar] [Publisher Link]

[15] T. Ruba et al., "Accurate Classification and Detection of Brain Cancer Cells in MRI and CT Images using Nano Contrast Agents," *Biomedical & Pharmacology Journal*, vol. 13, no. 3, pp. 1227-1237, 2020. [CrossRef] [Google Scholar] [Publisher Link]

[16] Nyoman Abiwinanda et al., "Brain Tumor Classification using Convolutional Neural Network," *World Congress on Medical Physics and Biomedical Engineering 2018*, Prague, Czech Republic, pp. 183-189, 2019. [CrossRef] [Google Scholar] [Publisher Link]

[17] Amin Kabir Anaraki, Moosa Ayati, and Foad Kazemi, "Magnetic Resonance Imaging-Based Brain Tumor Grades Classification and Grading via Convolutional Neural Networks and Genetic Algorithms," *Biocybernetics and Biomedical Engineering*, vol. 39, no. 1, pp. 63-74, 2019. [CrossRef] [Google Scholar] [Publisher Link]

[18] Parnian Afshar, Arash Mohammadi, and Konstantinos N. Plataniotis, "Brain Tumor Type Classification via Capsule Networks," *2018 25th IEEE International Conference on Image Processing (ICIP)*, Athens, Greece, pp. 3129-3133, 2018. [CrossRef] [Publisher Link]

[19] J. Seetha, and S. Selvakumar Raja, "Brain Tumor Classification using Convolutional Neural Networks," *Biomedical & Pharmacology Journal*, vol. 11, no. 3, pp. 1457-1461, 2018. [CrossRef] [Google Scholar] [Publisher Link]

[20] Rukiye Disci, Fatih Gurcan, and Ahmet Soylu, "Advanced Brain Tumor Classification in MR Images using Transfer Learning and Pre-Trained Deep CNN Models," *Cancers*, vol. 17, no. 1, pp. 1-21, 2025. [CrossRef] [Google Scholar] [Publisher Link]

[21] Anjana Bharati Subba, and Arun Kumar Sunaniya, "Computationally Optimized Brain Tumor Classification using Attention-Based GoogLeNet-Style CNN," *Expert Systems with Applications*, vol. 260, 2025. [CrossRef] [Google Scholar] [Publisher Link]

[22] Mohammad Amin et al., "DieT Transformer Model with PCA-ADE Integration for Advanced Multi-Class Brain Tumor Classification," *Intelligence-Based Medicine*, vol. 11, pp. 1-11, 2025. [CrossRef] [Google Scholar] [Publisher Link]

[23] Nadia Bibi et al., "A Transfer Learning-Based Approach for Brain Tumor Classification," *IEEE Access*, vol. 12, pp. 111218-111238, 2024. [CrossRef] [Google Scholar] [Publisher Link]

[24] Mohammed Aloraini et al., "Combining the Transformer and Convolution for Effective Brain Tumor Classification using Mri Images," *Applied Sciences*, vol. 13, no. 6, pp. 1-20, 2023. [CrossRef] [Google Scholar] [Publisher Link]

[25] Md Ishtyaq Mahmud, Muntasir Mamun, and Ahmed Abdelgawad, "A Deep Analysis of Brain Tumor Detection from MR Images using Deep Learning Networks," *Algorithms*, vol. 16, no. 4, pp. 1-19, 2023. [CrossRef] [Google Scholar] [Publisher Link]

[26] Gehad Abdullah Amran et al., "Brain Tumor Classification and Detection using Hybrid Deep Tumor Network," *Electronics*, vol. 11, no. 21, pp. 1-19, 2022. [CrossRef] [Google Scholar] [Publisher Link]

[27] Yurong Guan et al., "A Framework for Efficient Brain Tumor Classification using MRI Images," *Mathematical Biosciences and Engineering*, vol. 18, no. 5, pp. 5790-5815, 2021. [CrossRef] [Google Scholar] [Publisher Link]

[28] Neelum Noreen et al., "Brain Tumor Classification based on Fine-Tuned Models and the Ensemble Method," *Computers, Materials & Continua*, vol. 67, no. 3, pp. 3967-3952, 2021. [CrossRef] [Google Scholar] [Publisher Link]

[29] Raheleh Hashemzehi et al., "Detection of Brain Tumors from MRI Images based on Deep Learning using Hybrid Model CNN and NADE," *Biocybernetics and Biomedical Engineering*, vol. 40, no. 3, pp. 1225-1232, 2020. [CrossRef] [Google Scholar] [Publisher Link]

[30] S. Deepak, and P.M. Ameer, "Brain Tumor Classification using Deep CNN Features via Transfer Learning," *Computers in Biology and Medicine*, vol. 111, 2019. [CrossRef] [Google Scholar] [Publisher Link]

[31] Palash Ghosal et al., "Brain Tumor Classification using ResNet-101 Based Squeeze and Excitation Deep Neural Network," *2019 Second International Conference on Advanced Computational and Communication Paradigms (ICACCP)*, Gangtok, India, pp. 1-6, 2019. [CrossRef] [Google Scholar] [Publisher Link]

[32] Yufan Zhou et al., "Holistic Brain Tumor Screening and Classification based on Densenet and Recurrent Neural Network," *International MICCAI Brainlesion Workshop*, Granada, Spain, pp. 208-217, 2018. [CrossRef] [Google Scholar] [Publisher Link]

[33] Jenni A.M. Sidey-Gibbons, and Chris J. Sidey-Gibbons, "Machine Learning in Medicine: A Practical Introduction," *BMC Medical Research Methodology*, vol. 19, no. 1, pp. 1-18, 2019. [CrossRef] [Google Scholar] [Publisher Link]

[34] Shubhangi Solanki et al., "Brain Tumor Detection and Classification using Intelligence Techniques: An Overview," *IEEE Access*, vol. 11, pp. 12870-12886, 2023. [CrossRef] [Google Scholar] [Publisher Link]

[35] Emrah Irmak, "Multi-Classification of Brain Tumor MRI Images using Deep Convolutional Neural Network with Fully Optimized Framework," *Iranian Journal of Science and Technology, Transactions of Electrical Engineering*, vol. 45, no. 3, pp. 1015-1036, 2021. [CrossRef] [Google Scholar] [Publisher Link]

[36] Chirodip Lodh Choudhury et al., "Brain Tumor Detection and Classification using Convolutional Neural Network and Deep Neural Network," *2020 International Conference on Computer Science, Engineering and Applications (ICCSEA)*, Gunupur, India, pp. 1-4, 2020. [CrossRef] [Google Scholar] [Publisher Link]

[37] Wadhah Ayadi et al., "Deep CNN for Brain Tumor Classification," *Neural Processing Letters*, vol. 53, no. 1, pp. 671-700, 2021. [CrossRef] [Google Scholar] [Publisher Link]

[38] Arshia Rehman et al., "A Deep Learning-Based Framework for Automatic Brain Tumors Classification using Transfer Learning," *Circuits, Systems, and Signal Processing*, vol. 39, no. 2, pp. 757-775, 2020. [CrossRef] [Google Scholar] [Publisher Link]

[39] Hiba Mzoughi et al., "Deep Multi-Scale 3D Convolutional Neural Network (CNN) for MRI Gliomas Brain Tumor Classification," *Journal of Digital Imaging*, vol. 33, no. 4, pp. 903-915, 2020. [CrossRef] [Google Scholar] [Publisher Link]

[40] Jun Cheng, *Brain Tumor Dataset*, Figshare, 2017. [CrossRef] [Publisher Link]

[41] Ahmed Hamada, *Br35H: Brain Tumor Detection 2020*, Kaggle Datasets, 2020. [Publisher Link]

[42] Sartaj Bhuvaji et al., *Brain Tumor Classification (MRI)*, Kaggle Datasets, 2020. [Publisher Link]

[43] Zheshu Jia, and Deyun Chen, "Brain Tumor Identification and Classification of MRI Images using Deep Learning Techniques," *IEEE Access*, vol. 13, pp. 123783-123792, 2020. [CrossRef] [Google Scholar] [Publisher Link]

[44] A.R. Deepa, and W.R. Sam Emmanuel, "An Efficient Detection of Brain Tumor using Fused Feature Adaptive Firefly Backpropagation Neural Network," *Multimedia Tools and Applications*, vol. 78, no. 9, pp. 11799-1181, 2019. [CrossRef] [Google Scholar] [Publisher Link]

[45] Yun Jiang et al., "A Brain Tumor Segmentation New Method based on Statistical Thresholding and Multiscale CNN," *International Conference on Intelligent Computing*, Wuhan, China, pp. 235-245, 2018. [CrossRef] [Google Scholar] [Publisher Link]

[46] Yuexiang Li, and Linlin Shen, "Deep Learning-Based Multimodal Brain Tumor Diagnosis," *International MICCAI Brainlesion Workshop*, Granada, Spain, pp. 149-158, 2018. [CrossRef] [Google Scholar] [Publisher Link]

[47] Spyridon Bakas et al., "Advancing the Cancer Genome Atlas Glioma MRI Collections with Expert Segmentation Labels and Radiomic Features," *Nature Scientific Data*, vol. 4, no. 1, pp. 1-13, 2017. [CrossRef] [Google Scholar] [Publisher Link]

[48] Ahmed Al-Ashoor, Ferenc Lilik, and Szilvia Nagy, "A Systematic Analysis of Neural Networks, Fuzzy Logic and Genetic Algorithms in Tumor Classification," *Applied Sciences*, vol. 15, no. 9, pp. 1-23, 2025. [CrossRef] [Google Scholar] [Publisher Link]